catalysts

MDPI

Article

Ca-based Catalysts for the Production of High-Quality Bio-Oils from the Catalytic Co-Pyrolysis of Grape Seeds and Waste Tyres

Olga Sanahuja-Parejo, Alberto Veses, José Manuel López, Ramón Murillo, María Soledad Callén and Tomás García *

Instituto de Carboquímica (ICB-CSIC), C/ Miguel Luesma Castán, 50018 Zaragoza, Spain; osanahuja@icb.csic.es (O.S.-P.); a.veses@icb.csic.es (A.V.); jmlopez@icb.csic.es (J.M.L.); ramon.murillo@csic.es (R.M.); marisol@icb.csic.es (M.S.C.)

* Correspondence: tomas@icb.csic.es

Received: 31 October 2019; Accepted: 22 November 2019; Published: 26 November 2019

Abstract: The catalytic co-pyrolysis of grape seeds and waste tyres for the production of high-quality bio-oils was studied in a pilot-scale Auger reactor using different low-cost Ca-based catalysts. All the products of the process (solid, liquid, and gas) were comprehensively analysed. The results demonstrate that this upgrading strategy is suitable for the production of better-quality bio-oils with major potential for use as drop-in fuels. Although very good results were obtained regardless of the nature of the Ca-based catalyst, the best results were achieved using a high-purity CaO obtained from the calcination of natural limestone at 900 °C. Specifically, by adding 20 wt% waste tyres and using a feedstock to CaO mass ratio of 2:1, a practically deoxygenated bio-oil (0.5 wt% of oxygen content) was obtained with a significant heating value of 41.7 MJ/kg, confirming its potential for use in energy applications. The total basicity of the catalyst and the presence of a pure CaO crystalline phase with marginal impurities seem to be key parameters facilitating the prevalence of aromatisation and hydrodeoxygenation routes over the de-acidification and deoxygenation of the vapours through ketonisation and esterification reactions, leading to a highly aromatic biofuel. In addition, owing to the CO_2-capture effect inherent to these catalysts, a more environmentally friendly gas product was produced, comprising H_2 and CH_4 as the main components.

Keywords: co-pyrolysis; biomass; waste tyres; bio-oils; Ca-based catalyst; auger reactor

1. Introduction

The bio-oil produced from lignocellulosic biomass pyrolysis has outstanding potential as a renewable source of green energy and chemicals [1]. It should also be mentioned that several companies have implemented the commercial stages for bio-oil production [2]. However, an attractive market for this liquid product is not yet available [3], and it is still necessary to facilitate the standardisation and commercialisation of these liquid bio-oils [4]. Interestingly, the first insights into the application of this liquid as a drop-in fuel have shown great potential, increasing its market opportunities [5,6]. However, the complex nature of the bio-oil poses challenges for its competitive incorporation into the current energy market, particularly given its excessive content in reactive oxygen compounds, which affect both its handling and storage, and therefore, limiting its value for consideration as a drop-in fuel in current energy infrastructure. To overcome these limitations, upgrading methods such as hydrodeoxygenation, catalytic cracking, fast catalytic pyrolysis, hydrogenation, and molecular distillation are considered the most promising strategies to reach this aim [7]. Interestingly, due to their potential economic advantages and moderate operating conditions, catalytic processes focused on the in-situ cracking of this bio-oil are emerging as a potentially effective method to achieve this [8].

Zeolites are the main type of catalysts studied for this purpose [9,10]. In general terms, the main drawback of using these high-cost materials lies in catalyst deactivation, essentially the result of zeolite coking. Although zeolite regeneration may be carried out by char combustion in an integrated process [11,12], the high combustion temperatures required (above 700 °C), together with the presence of steam (approximately 10% in volume), would restrict their use in industrial processes due to their long-time deactivation by partial dealumination. Hence, the search for low-cost catalysts [13] must be considered as a promising economically viable strategy to compete in the current energy market. Basic catalysts such as MgO or calcium-based materials are emerging as attractive and relatively economical catalysts with which to carry out catalytic pyrolysis [13–15]. In this regard, Kalogiannis et al. [16] evaluated the fast catalytic pyrolysis of commercial lignocellulosic biomass at a representative scale using a circulating fluidised-bed facility with MgO catalysts and commercial zeolites. These authors found that ketonisation and aldol condensation reactions were promoted by the basic sites of MgO, resulting in a hydrogen-rich bio-oil being produced. In another interesting study conducted by our research group in a pilot auger reactor plant, calcined calcite and calcined dolomite were evaluated as catalysts for use in a self-sustained energy system. The oxygen fraction and acidic character of the bio-oil were decreased in both cases, while pH and calorific values were increased. Unfortunately, these bio-oils still require a further upgrading step if they are to be contemplated as a real substitute for fossil fuels or even as a drop-in fuel.

New alternative strategies such as the incorporation of polymer residues into conventional pyrolysis processes have also been considered in recent years. Detailed information on the latest advances in this process can be found in different exhaustive reviews [17–19]. In particular, the addition of waste tyres [20–22] and different plastic waste such as polystyrene [23], polyethylene [24], and polypropylene [25] to lignocellulosic biomass was studied as a potential route to improving the properties of the bio-oil, both by decreasing oxygen content and increasing heating value [26]. In this case, waste plastics acted as hydrogen donors by promoting oligomerisation, cycling, and hydrodeoxygenation reactions. Again, there is general consensus, mainly owing to its high viscosity, water content, oxygen content, acidic nature, solid, and ash content, and non-homogenous nature, that a further upgrading step is still necessary to facilitate the incorporation of this bio-oil obtained by co-pyrolysis processes into the energy market, especially for use as drop-in fuels.

Thus, a combined strategy involving the catalytic co-pyrolysis of lignocellulosic biomass with polymer waste has emerged as a very promising solution for the production of drop-in fuels in a simple, one-step process. Recent progress in this strategy can be found in different extensive reviews [27–29]. The catalysts successfully studied for this purpose were mainly zeolites (HY and HZSM-5), mesoporous materials (MCM-41 and SBA-15), alumina, spent Fluid Catalytic Cracking (FCC) catalysts, and a number of minerals, such as bentonite. Interestingly, our research group was also able to demonstrate the potential of this process to facilitate the production of drop-in fuels in a laboratory-scale fixed-bed reactor. Particularly, the catalytic co-pyrolysis of grape seeds (GSs), as a form of agricultural waste, and waste tyres (WTs) was successfully carried out using calcined limestone as the catalyst [30]. Thus, this combined strategy made it feasible to produce a deoxygenated and aromatic-rich drop-in fuel by applying one simple stage. More specifically, the positive effects attached to CaO were not only responsible for promoting the dehydration and dehydrogenation reactions of acids and phenols, but also for the production of a more environmentally friendly gas because of the in-situ CO_2-capture effect associated with CaO carbonation. Although the results of catalytic co-pyrolysis are very encouraging, most of the work in this field has been carried out in micro and lab-scale reactors [31–37], and the demonstration of this process on a larger scale is still limited [38]. Therefore, the study of this upgrading strategy to a larger scale (Technology Readiness Levels, TRL ≥ (5)) seems necessary as a first step towards the implementation of the catalytic co-pyrolysis processes of lignocellulosic biomass with waste plastics in future bio-refineries. In this sense, the use of auger reactors at TRL-5 have shown to be a robust and flexible option for pyrolysis processes [15,39–42]. However, further experimental research is required to verify the proposed approaches in a relevant environment. Specifically, to the best of our

knowledge, there is no published data on catalytic co-pyrolysis using both of these feedstocks (grape seeds and waste tyres) on a relevant scale that could contribute to validating the potential of these upgraded bio-oils.

Thus, the aim of this work is to demonstrate the potential of the catalytic co-pyrolysis of waste tyres and grape seeds for the production of improved bio-oils in a relevant environment (TRL-5). For this purpose, the experiments were conducted in an Auger reactor pilot plant operating at atmospheric pressure. GSs and WTs (up to 20 wt%) were used as feedstock. Four Ca-based materials obtained from different companies were studied as low-cost commercial catalysts.

2. Results

2.1. Characterisation of Catalysts

The purity and crystallinity of each catalyst was verified by X-ray diffraction (XRD), see Figure 1. It is worth mentioning that while the Ca-based-1, Ca-based-2, and Ca-based-3 catalysts were obtained from limestone calcination at 900 °C, the Ca-based-4 catalyst was obtained from dolomite calcination at the same temperature. Accordingly, it can be observed that the Ca-based-1, Ca-based-2, and Ca-based-3 catalysts mainly presented the characteristic diffraction peaks of calcium oxide. These peaks were situated at 2θ 33°, 38°, 53°, 63°, and 68°, corresponding to the crystallographic planes (111), (200), (202), (311), and (222), respectively [43,44]. Diffraction patterns also showed diffraction peaks related to $Ca(OH)_2$, which could be associated with the fact that water was absorbed from the environment during handling [45], which is more significant in the case of the Ca-based-3 catalyst. The presence of magnesium calcite cannot be ruled out in this sample. Finally, CaO and MgO diffraction peaks were identified for the Ca-based-4 catalyst, in line with the use of dolomite as its raw mineral. Diffraction peaks could also be observed at 2θ 23°, 29°, 40°, and 48°, corresponding to the structure of magnesium calcite and highlighting that 900 °C was not a high enough temperature to ensure the total decomposition of this phase during the pre-calcination step. Finally, $Ca(OH)_2$ was also identified as a minor phase. It is worth mentioning that while these hydroxides were again transformed into the metal oxide under pyrolysis conditions, the opposite was true in the case of magnesium calcite.

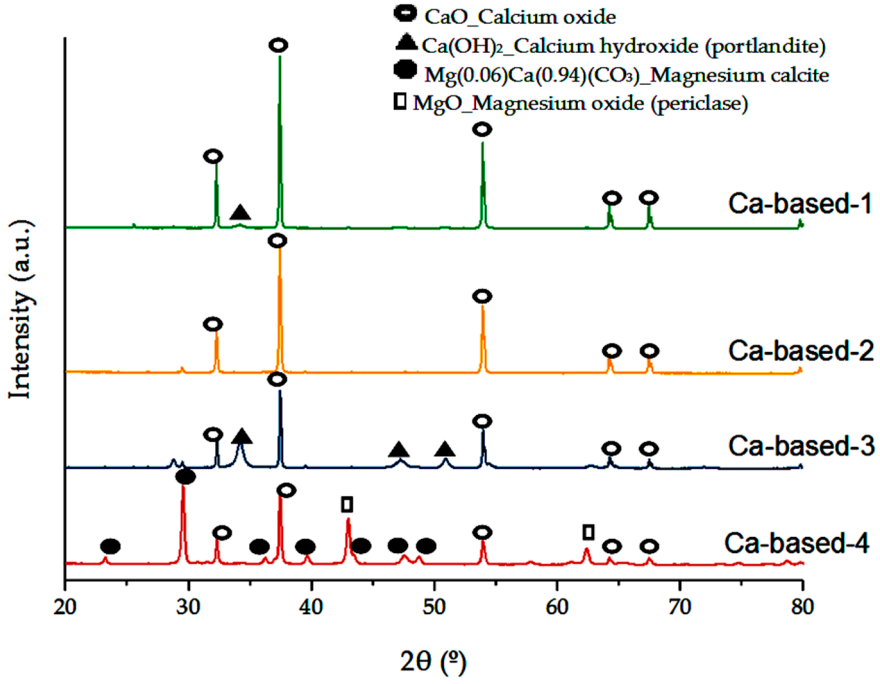

Figure 1. XRD patterns of the different Ca-based catalysts.

Table 1 shows the elemental composition of the different Ca-based catalysts as determined by inductively coupled plasma-optical emission spectrometry (ICP-OES). As expected, the main elements were Ca and Mg. The remaining elements found in the catalysts were identified in quantities lower than 1.0 wt% (Al, Fe, K, S, and Si). As could be expected, the highest MgO content was identified in the Ca-based-4 catalyst (47.6 wt%), while the remaining catalysts showed lower MgO content, between 0.33-0.86 wt%. The high purity of the Ca-based-1 catalyst should be pointed out since CaO was present in a very high percentage, 95 wt%. For the different catalysts, Ca content in the order from higher to lower was as follows: Ca-based-1 > Ca-based-2 > Ca-based-3 > Ca-based-4. Table 1 also shows that all the Ca-based catalysts displayed quite a low specific surface area, with this being slightly higher in the case of the catalyst obtained from dolomite. It is also worth highlighting that the average pore diameter of the Ca-based-4 catalyst ranged between 2 and 50 nm, which corresponded to a mesoporous structure according to the International Union of Pure and Applied Chemistry (IUPAC) classification. The remaining catalysts (Ca-based-1, Ca-based-2, Ca-based-3) had an average pore diameter >50 nm, which indicated a macroporous structure. With regards to porosity values, no significant differences were observed since values remained in the range of 42–53% for all the catalysts.

Table 1. ICP-OES and the structural characterisation of the Ca-based catalysts. BET and D_p determined by N_2 adsorption. Porosity was determined by Hg porosimetry.

	CaO (wt%)	MgO (wt%)	Al_2O_3 (wt%)	Fe_2O_3 (wt%)	K_2O (wt%)	SiO_2 (wt%)	BET (m^2/g)	D_p (nm)	Porosity (%)
Ca-based-1	95.1 ± 0.7	0.86 ± 0.03	0.14 ± 0.01	0.29 ± 0.02	0.02 ± 0.00	0.51 ± 0.02	< 2	520	50
Ca-based-2	89.8 ± 0.6	0.78 ± 0.03	0.14 ± 0.01	0.10 ± 0.01	0.15 ± 0.01	1.09 ± 0.04	5	428	42
Ca-based-3	79.8 ± 0.4	0.33 ± 0.02	0.14 ± 0.01	0.07 ± 0.00	0.04 ± 0.00	0.60 ± 0.00	6	192	53
Ca-based-4	47.6 ± 0.2	33.2 ± 0.10	0.08 ± 0.00	–	0.02 ± 0.00	0.24 ± 0.01	12	48	50

The acidity of the Ca-based catalysts was studied with the TPD-NH_3 technique, using a mass spectrometer as a detector, and values of desorbed μmolNH_3/g were calculated by dividing the area of the peak between the mass of the treated sample. Those values were included in Table 2.

Table 2. Amount of CO_2 and NH_3 desorbed from the TPD-CO_2 and TPD-NH_3 profiles of the different catalysts.

	Ca-based-1	Ca-based-2	Ca-based-3	Ca-based-4
molNH_3/g (T Peak (°C))	0.2 (630)	0.1 (650)	0.3 (690)	0.8 (750)
mmolCO_2/g (T Peak (°C))	0.04 (550)	0.10 (562)	0.10 (592)	0.11 (598)

Figure 2 shows a quantitative analysis of the desorbed NH_3 based on the fragment m/z = 15 for the different Ca-based catalysts. Values were quite small (ranging between 0.1 and 0.8 μmolNH_3/g), in line with the marginal acidity also observed by other researchers using similar catalysts [13]. The Ca-based-4 catalyst was the solid with the highest amount of acid sites, suggesting that these strong acid sites could be linked to the presence of magnesium calcite. Accordingly, a slightly lower acidity can be seen for the Ca-based-3 catalyst, while the Ca-based-1 and Ca-based-2 catalysts presented the lowest values.

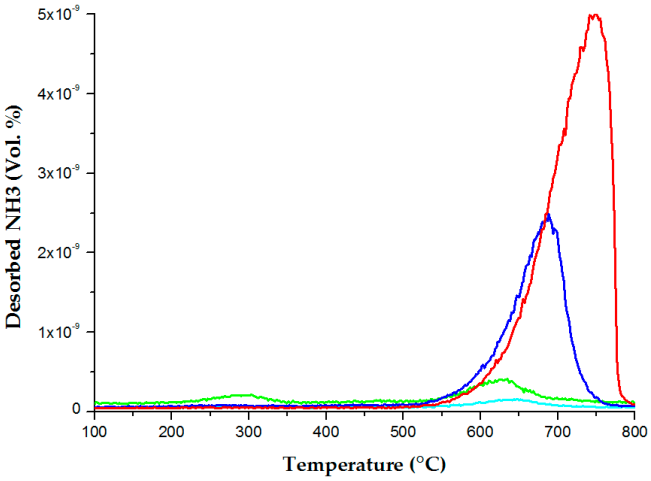

Figure 2. Quantitative analysis of the desorbed NH_3 referenced to the fragment m/z = 15. Ca-based-1 (green), Ca-based-2 (cyan), Ca-based-3 (blue), and Ca-based-4 (red).

TPD-CO_2 technique was performed to know the basicity of the Ca-based catalysts. These basic sites can play an important role as active centres in such specific deoxygenation reactions [46] as esterification and ketonisation. As an example, and for simplification, the TPD-CO_2 profile of the Ca-based-1 catalyst was plotted in Figure 3. Similar strength of the basicity sites was observed for all the catalysts showing CO_2 desorption temperatures of 550–600 °C. More importantly, the Ca-based-1 catalyst showed the lowest amount of evolved CO_2, 0.04 mmolCO_2/g, whereas comparable higher values of 0.10–0.11 mmolCO_2/g were found for the other materials (see Table 2). The lower specific surface area observed in the Ca-based-1 catalyst could explain its lower total basicity [13,47].

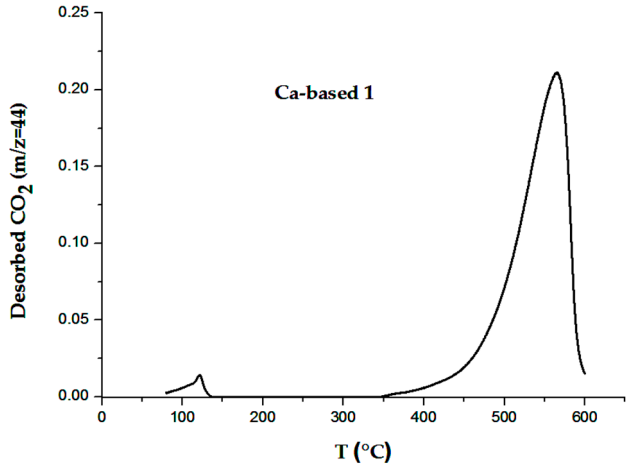

Figure 3. TPD-CO_2 profile of the Ca-based-1 catalyst (fragment m/z = 44).

2.2. Product Yields

To evaluate the importance of the addition of WTs on the distribution of the products, different mixtures of GSs and WTs (10 and 20 wt%) were treated in an auger pilot plant. Yields obtained from the pyrolysis of both raw materials are also shown in Table 3 for comparative purposes. Thus, the liquid yield derived from GSs was 42.5 wt%, while the solid and gas yields were 31.2 and 23.2 wt%, respectively. On the other hand, the pyrolysis of WTs generated a lower liquid yield (37.8 wt%) and a comparable gas fraction (23.5 wt%), leading to a higher solid yield (37.5 wt%). These values could be considered in line with other work related to WT pyrolysis in auger reactors [40]. According to these values, the addition of WTs to GSs follows an expected trend in the distribution of products. Thus, the

liquid yield decreased with respect to GSs. Correspondingly, the solid yields were higher, and gas yields were close to those obtained in biomass pyrolysis and WTs pyrolysis.

Table 3. Product yields (liquid, solid, and non-condensable gas) and liquid phase distribution (organic and aqueous phases) obtained after the pyrolysis and co-pyrolysis experiments carried out in the Auger pilot plant. Catalytic co-pyrolysis experiments were carried out, adding 20 wt% of waste tyres. Values were determined as the average of two runs.

	Liquid (wt%)		Solid (wt%)			Gas	Balance	Phase Distribution (wt%)	
	Org.	Aq.	Char	Coke	CO_2			Org.	Aq.
GSs	16.0 ± 0.8	26.5 ± 1.3	31.2 ± 1.6	0	0	23.2 ± 1.2	96.9	37.7	62.3
WTs	37.8 ± 1.9	0.0 ± 0.0	37.5 ± 1.8	0	0	23.5 ± 1.2	98.8	100.0	0.0
GSs/WTs (90/10)	12.8 ± 0.6	20.2 ± 1.0	36.7 ± 1.2	0	0	28.9 ± 1.5	98.5	38.9	61.1
GSs/WTs (80/20)	17.4 ± 0.8	18.2 ± 0.9	35.4 ± 1.8	0	0	24.2 ± 1.2	95.1	48.8	51.2
Ca-based-1	15.7 ± 0.8	23.0 ± 1.2	34.6 ± 1.7	0.37	1.8	20.5 ± 1.0	95.2	40.6	59.4
Ca-based-2	15.8 ± 0.8	21.4 ± 1.1	37.7 ± 1.9	0.39	1.6	19.7 ± 1.0	96.6	42.4	57.6
Ca-based-3	15.7 ± 0.8	20.6 ± 1.0	37.2 ± 1.8	0.41	2.4	20.1 ± 1.0	96.4	43.2	56.8
Ca-based-4	16.8 ± 0.9	20.0 ± 1.0	37.6 ± 1.9	0.41	2.6	18.7 ± 0.9	96.2	45.6	54.4

With regard to GS pyrolysis, the liquid fraction resulting from the non-catalytic co-pyrolysis process was composed of two phases (aqueous and organic), which were easily separated by centrifugation. While the organic phase is the most interesting fraction for use in fuel and energy applications [48], the possibilities for valorising the aqueous phase are still limited, given that the production of chemical products such as H_2, ethanol or even light acids is the option attracting more interest. Accordingly, the main target of this study was focused on improving the yield and fuel properties of the organic phase. Interestingly, the yield to this fraction only increased with the highest WT percentage (20 wt%), reaching values up to 10% higher, approximately. This behaviour was also observed in previous co-pyrolysis work where the addition of polymer waste to the biomass pyrolysis process enhanced the yield to the organic fraction [18,27].

Several catalytic tests using the Ca-based-1 catalyst were carried out using GSs and WTs on their own. Since no significant improvement was evidenced, the resulting information was only included as supporting information (Tables S1 and S2). Subsequently, the catalytic co-pyrolysis of GSs and WTs using low-cost Ca-based materials was studied at TRL-5. We would point out here that a ratio (GSs + WTs) to catalyst of 2 was selected, since we had previously observed that higher catalyst ratios excessively promoted cracking reactions, leading to the formation of undesired heavy condensable organic compounds [49,50]. On the other hand, the use of lower catalyst proportions in the feedstock hardly affected process performance compared to the non-catalytic test. Table 3 compiles the result obtained for the different GS and WT catalytic co-pyrolysis tests. Liquid yields are observed to range between 36.8 and 38.0 wt%, slightly higher in comparison with non-catalytic experiments. Interestingly, organic fraction yields were only slightly lower in comparison with the non-catalytic tests, remaining in the same range of values for all the catalytic experiments. This fact could be explained by the promotion of dehydration reactions by Ca-based materials, eventually increasing the yield to the aqueous fraction. This tendency has also been observed by other researchers [51]. For these catalytic tests, the solid yield was separated into char, CO_2 (as carbonate), and coke yields (by TGA analysis). As can be observed in Table 3, the effect of CaO carbonation is evident after the experiments, while remarkably low values of coke yield (0.37–0.41 wt%) were achieved. Slightly higher carbonation was observed in those Ca-based materials where Magnesium calcite phase was observed by XRD since this phase could be decarbonated under TGA conditions. In addition, gas yields were slightly lower after the catalytic experiments in comparison with the non-catalytic tests.

2.3. Upgraded Bio-Oil: Analysis of the Organic Fraction Properties

Since the main target in this work was to improve the quality of the organic fraction, this product was comprehensively characterised. Table 4 summarises the main properties of this fraction. First, it can be seen that the organic phase obtained from GS pyrolysis had a remarkably high water content (5.09

wt%), whereas the water content of the WT pyrolytic oil was practically negligible. Correspondingly, the water content of the organic fraction was drastically reduced by adding WTs to the feedstock, especially at 20 wt% (1.07 wt%). Focusing on the catalytic experiments (see Table 4), the exceptional performance of Ca-based catalysts can be highlighted, with the water content in the organic fraction decreasing to values lower than 1 wt%. Other important physical properties of the organic phase as a liquid fuel, such as density and viscosity, were also determined [52]. While the organic fraction from GS pyrolysis is a viscous liquid (87.1 mPa.s) with higher density (1.30 g/mL) than commercial fuels [53,54], organic WTs pyrolytic oil can be considered similar to fossil fuel-derived oils, showing a viscosity of 3.2 mPa.s and a density of 0.87 g/mL. In this regard, positive effects on these physical properties can be directly obtained through to the addition of WT to the feedstock. Accordingly, viscosity and density values were reduced down to 21.3–16.3 mPa.s and 1.15–1.11 g/mL, respectively, depending on the WT percentage in the feedstock. These findings were in line with the results found by Cao et al. [55], which showed that there was an improvement in these physical properties when the co-pyrolysis of pine sawdust and waste tyres was carried out in a fixed-bed reactor. Significantly, these positive effects were further improved when Ca-based catalysts were incorporated into the process [56]. Thus, a remarkable reduction in the parameters of viscosity and density was achieved, leading to values lower than 6 mPa.s and 1 g/mL, respectively, for all the catalysts. Specifically, the Ca-based-1 catalyst produced the organic fraction with the lowest water content (0.62 wt%) and the best physical properties as a fuel (υ = 3.5 mPa.s; ρ = 0.91 (g/mL), which were seen as very remarkable achievements.

Table 4. Organic fraction properties after the pyrolysis, co-pyrolysis, and catalytic co-pyrolysis processes. Deox.: deoxygenation; LHV: lower heating value.

	Properties				Elemental Analysis (wt%)						
	H2O (wt%)	pH	υ (mPa.s)	ρ (g/mL)	C	N	H	S	O	Deox. (%)	LHV (MJ/kg)
GSs	5.09 ± 0.7	8.0	87.1 ± 2.6	1.30	77.4 ± 0.8	2.5 ± 0.2	8.3 ± 0.2	0.2 ± 0.02	11.6 ± 0.6	–	34.6 ± 1.0
WTs	<0.3 ± 0.0	8.3	3.2 ± 0.2	0.87	89.9 ± 1.0	1.1 ± 0.1	7.6 ± 0.1	0.7 ± 0.03	0.7 ± 0.1	–	42.4 ± 1.3
GSs/WTs (90/10)	4.83 ± 0.6	9.6	21.3 ± 1.2	1.15	80.6 ± 0.9	2.8 ± 0.2	8.3 ± 0.2	0.6 ± 0.03	7.8 ± 0.5	32.8	36.0 ± 1.4
GSs/WTs (80/20)	1.07 ± 0.1	9.5	16.3 ± 0.8	1.11	83.6 ± 0.9	2.6 ± 0.2	9.5 ± 0.2	0.4 ± 0.02	3.9 ± 0.2	66.4	38.78 ± 1.2
Ca-based-1	0.62 ± 0.1	9.1	3.5 ± 0.2	0.91	87.0 ± 0.8	2.5 ± 0.1	9.6 ± 0.2	0.4 ± 0.02	0.5 ± 0.1	95.7	40.7 ± 1.5
Ca-based-2	0.70 ± 0.1	8.9	4.7 ± 0.2	0.95	85.5 ± 0.7	2.7 ± 0.2	10.2 ± 0.3	0.6 ± 0.03	1.1 ± 0.2 0.3	90.5	40.7 ±1.5
Ca-based-3	0.90 ± 0.1	9.1	5.5 ± 0.3	0.97	85.0 ± 0.7	2.7 ± 0.2	9.9 ± 0.2	0.5 ± 0.02	1.9 ± 0.3	83.6	40.3 ±1.4
Ca-based-4	0.76 ± 0.1	9.1	5.6 ± 0.3	0.98	84.9 ± 0.4	2.8 ± 0.2	10.0 ± 0.1	0.6 ± 0.03	1.8 ± 0.2	84.5	40.1 ± 1.4

Another important parameter to measure the quality of the liquid is acidity. In this case, acidity was measured by pH determination. Interestingly, the GS-derived organic fraction presented a pH value of 8, preventing the presence of the corrosion issues associated with the handling and storage of the highly acidic bio-oils usually obtained from lignocellulosic biomass (pH 3–4). This value was in the range of other pyrolytic oils obtained from GSs, probably due to the presence of a remarkable amount of basic N-derived compounds in the feedstock [26,30]. The pH value for WT-derived oil was quite similar (8.3). It is worth highlighting that both co-pyrolysis and catalytic co-pyrolysis bio-oils only entailed a slight increase in pH values, while still preserving an appropriate value (8.9–9.6) for handling and storage purposes.

In relation to the elemental analysis, it could be also seen that the bio-oil derived from the pyrolysis of GSs contained 11.6 wt% of oxygen. Although it could be still considered a remarkable oxygen content for its further direct utilisation as a drop-in fuel, this value was quite low when compared to those found in bio-oils produced from the pyrolysis of other types of lignocellulosic biomass [14,57,58]. This result confirmed that those lignocellulosic agricultural wastes were exceptional alternatives to be used in the pyrolysis process. On the contrary, pyrolytic WT oil presented insignificant amounts of oxygen (<1 wt%). Obviously, the incorporation of WT led to a better-quality bio-oil in relation to lower oxygen content. It should be highlighted that this improvement was always better than that expected according to the rule of mixtures. Specifically, it was possible to reduce the oxygen content down to 3.9 wt% by adding up to 20 wt% of WTs. The effect of catalyst addition on the deoxygenation process

was more apparent. Oxygen contents in the upgraded bio-oils were always lower than 2 wt%, reaching the lowest value of 0.5 wt% with the Ca-based-1 catalyst. In this sense, although the formation of H_2O soluble compounds cannot totally be ruled out, retention of CO_2 and H_2O seems to be enhanced by these catalysts. At this point, it should be pointed out that the elemental composition of the aqueous fraction was also determined (Table S3, supplementary data). The values of carbon content determined were quite similar and were in the range of 4.14–6.53 wt%, where small differences can be attributed to experimental error. Thus, these results suggest that a great effect of the catalysts is produced in improving the organic fraction since no additional organic components seem to be dissolved in the aqueous fraction.

Hence, a practically deoxygenated organic fraction was produced (values of deoxygenation in range of 83.6–95.7%), entailing significant lower heating values (LHVs) of about 40–41 MJ/kg. Although all the catalysts led to very good results, again, it is worth highlighting the performance of the Ca-based-1 catalyst, which produced the best organic oil in terms of lower oxygen content and LHV.

2.4. Non-Condensable Gas Composition

Table 5 summarises the non-condensable gas composition after pyrolysis, co-pyrolysis, and catalytic co-pyrolysis reactions. It can be observed that, in the case of GS pyrolysis, the composition of this gas was rich in CO_2 (10.5 g/100 g feedstock), and also in CO (3.1 g/100 g feedstock) and CH_4 (5.5 g/100 g feedstock). The remaining C_2-C_4 hydrocarbons were present as marginal content. In the case of pyrolysis of WTs, hydrogen and methane were the main gases, since CO and CO_2 were produced in lower amounts, as could be expected by the low oxygen content present in WTs. When WTs were added to the feed, there was a decrease in CO_2 in the gas stream and a slight increase in CH_4 and H_2. As a consequence, a more valuable non-condensable gas in terms of LHV was produced as the WT ratio in the feedstock was increased from 10 to 20 wt%, 28.5, and 30.3 MJ/Nm^3, respectively. By adding the catalyst to the GS/WT mixture, significant positive differences were seen in the composition of the gas. First, it can be highlighted the meaningful increase regarding the production of hydrogen and methane, and the significant reduction in the CO_2 emitted. This reduction in CO_2 can be explained assuming that CaO is a CO_2 sorbent. This reaction favours the production of hydrogen caused by the enhancement of the water gas shift reaction, which in turn affects the reaction of methane reforming [15]. Accordingly, a direct relationship can be found between the amount of CO_2 in the gas fraction and the CaO content in the catalysts, with the Ca-based-1 and Ca-based-4 catalysts leading to the lowest and highest amounts of CO_2 in the gas fraction, respectively. The poor performance of the Ca-based-4 catalyst was not surprising since it is well known that MgO in Ca-based sorbents does not significantly contribute to CO_2 capture at such temperature [15]. Additionally, some Magnesium calcite phase was detected, which cannot contribute to this process. Another positive effect of incorporating Ca-based catalysts was found in the increase in heating value. Thus, by means of the addition of these types of solids, it was possible to enhance heating values up to 40 MJ/Nm^3, approximately. Interestingly, emissions of H_2S in the catalytic co-pyrolysis processes were comparable to those obtained during the GS pyrolysis, which may be associated with the desulphuration capacity of Ca-based materials.

Table 5. Lower heating value (LHV) (MJ/Nm^3) and non-condensable gas composition (g/100 g feedstock) produced after the pyrolysis, co-pyrolysis, and catalytic co-pyrolysis processes.

Experiment	H_2	CO_2	CO	CH_4	C_2H_6	C_2H_4	C_3-C_4	H_2S	LHV (MJ/Nm^3)
GSs	0.21 ± 0.01	10.5 ± 0.60	3.1 ± 0.16	5.5 ± 0.31	0.8 ± 0.05	1.1 ± 0.06	1.9 ± 0.10	0.02	24.1 ± 1.2
WTs	0.34 ± 0.03	0.65 ± 0.06	0.21 ± 0.02	10.2 ± 0.60	2.1 ± 0.16	1.7 ± 0.14	8.1 ± 0.65	0.25	53.6 ± 2.0
GSs/WTs(90/10)	0.21 ± 0.02	7.9 ± 0.40	2.5 ± 0.13	5.3 ± 0.32	0.9 ± 0.10	1.1 ±.0.09	2.5 ± 0.25	0.04	28.5 ± 1.4
GSs/WTs(80/20)	0.22 ± 0.02	7.07 ± 0.40	2.2 ± 0.12	5.5 ± 0.35	0.9 ± 0.10	1.1 ± 0.09	2.7 ± 0.35	0.04	30.3 ± 1.5
Ca-based-1	0.31 ± 0.03	2.42 ± 0.12	3.2 ± 0.16	7.3 ± 0.45	1.5 ± 0.12	1.2 ± 0.12	4.3 ± 0.40	0.00	39.3 ± 1.8
Ca-based-2	0.33 ± 0.03	1.7 ± 0.09	3.0 ± 0.15	7.1 ± 0.40	1.3 ± 0.11	1.1 ± 0.10	4.2 ± 0.35	0.00	39.8 ± 1.8
Ca-based-3	0.33 ± 0.02	1.9 ± 0.10	3.3 ± 0.17	7.3 ± 0.40	1.4 ± 0.14	1.1 ± 0.09	4.5 ± 0.42	0.02	39.9 ± 1.9
Ca-based-4	0.19 ± 0.01	5.34 ± 0.35	3.2 ± 0.16	6.4 ± 0.38	1.3 ± 0.12	1.0 ± 0.11	4.1 ± 0.34	0.02	37.0 ± 1.7

2.5. GC-MS

A semi-quantitative identification of the compounds (relative area percentage, r.a.%) found in the organic phase was performed using gas chromatography-mass spectrometry (GC-MS). Table 6 summarises the chemical composition of the organic fractions derived from the pyrolysis, co-pyrolysis, and catalytic co-pyrolysis processes. The chemical composition of the organic fraction obtained after the GS pyrolysis was composed mainly of oxygenated compounds (phenols, esters, fatty acids, aromatics, ketones, cyclic hydrocarbons, olefins, and other oxygenated compounds) [59,60]. It should be pointed out that these compounds were already identified in previous work as the main oxygenated compounds in the organic fraction of the bio-oil obtained from the pyrolysis of grape seeds [24,30]. Interestingly, a noteworthy amount of aromatic compounds was also identified (31.6%). On the other hand, the organic fraction of the pyrolysis liquid of WTs presented a prevailing fraction of aromatics (more than 90 r.a.%), followed by a significant proportion of cyclic hydrocarbons (6.2 r.a.%). The more relevant aromatic components of the liquid fraction were also identified, which were benzene and benzene-derived compounds (toluene, xylene, ethyl-benzene, and styrene) [61]. A list of the main identified components can be found in the supporting information in Tables S4 and S5. It can be observed in Table 6 that in the case of GS/WT co-pyrolysis, a considerable increase in cyclic and aromatic hydrocarbon production was achieved in comparison with GS pyrolysis. A remarkable reduction in oxygenated compounds, mainly esters but also phenols and fatty acids, was observed at the same time. These tendencies may be associated with the promotion of hydrodeoxygenation reactions due to the H_2-donor effect of the WTs [3]. For more information on the compounds identified after the co-pyrolysis process, see Table S6, supplementary data.

Table 6. Chemical composition of bio-oils derived from the pyrolysis, co-pyrolysis, and catalytic co-pyrolysis processes as the percentage of the relative area (r.a.%). HC: Hydrocarbons; OC: Oxygenated Compounds. Catalytic co-pyrolysis experiments were carried out, adding 20 wt% of waste tyres.

Experiment	Aromatics	Olefins	Linear HC	Cyclic HC	Phenols	Esters	Ketones	Fatty Acids	Others OC
GSs	31.6 ± 2.5	7.6 ± 0.6		–	18.8 ± 1.5	28.7 ± 2.3	0.8 ± 0.3	7.4 ± 0.3	5.1 ± 0.2
WTs	91.8 ± 2.5	–		8.2 ± 0.5	–	–	–	–	–
GSs/WTs (90/10)	63.3 ± 2.6	2.9 ± 0.3	0.4 ± 0.2	23.0 ± 1.2	6.4 ± 0.8	0.9 ± 0.2	0.1 ± 0.0	1.1 ± 0.2	1.9 ± 0.2
GSs/WTs (80/20)	64.3 ± 2.8	2.8 ± 0.3	0.4 ± 0.2	24.0 ± 1.5	4.9 ± 0.5	0.8 ± 0.2	0.1 ± 0.0	1.1 ± 0.2	1.8 ± 0.2
Ca-based-1	70.9 ± 2.9	2.3 ± 0.2	0.6 ± 0.3	16.0 ± 0.8	1.3 ± 0.3	1.5 ± 0.2	2.0 ± 0.1	1.7 ± 0.3	3.6 ± 0.4
Ca-based-2	60.4 ± 2.2	4.1 ± 0.5	1.8 ± 0.4	16.1 ± 0.9	2.8 ± 0.6	2.6 ± 0.3	5.0 ± 0.7	2.5 ± 0.4	4.1 ± 0.5
Ca-based-3	54.5 ± 2.0	5.7 ± 0.8	2.8 ± 0.5	18.0 ± 1.0	2.8 ± 0.6	3.2 ± 0.4	6.2 ± 0.8	2.7 ± 0.5	4.0 ± 0.4
Ca-based-4	58.3 ± 2.2	5.0 ± 0.6	1.6 ± 0.3	18.3 ± 1.0	3.9 ± 0.3	2.9 ± 0.3	5.0 ± 0.7	2.4 ± 0.4	4.0 ± 0.4

The chemical composition of the organic fractions obtained in the catalytic co-pyrolysis experiments is also shown in Table 6. A different composition to that analysed in the bio-oil of the GS pyrolysis run was clearly identified. As in the case of the co-pyrolysis test, a notable reduction in the phenol, ester, and fatty acid contents were achieved, while aromatics, olefins, linear paraffins, and cyclic hydrocarbons were significantly increased. Therefore, this behaviour could be again related to the prevalence of aromatisation and hydrodeoxygenation reactions owing to the significant amount of H_2 produced by both the thermal cracking of WTs and the water gas shift reaction assisted by CaO. These results were in line with the low oxygen content and the marginal amount of water found in these liquids. With regard to the effect of the catalyst on process performance, a slightly different organic fraction composition was evidenced depending on the Ca-based material. There was generally observed to be a reduction in the cyclic-hydrocarbon composition compared to the non-catalytic process. This fact, together with a remarkable increase in ketones, pointed to the cascade of reactions associated with the hydrodeoxygenation of ketones in order to favour cyclic-hydrocarbon production not being fully accomplished. Accordingly, another important deoxygenation route during the catalytic co-pyrolysis experiments seemed to be decarboxylation. This behaviour was in line with previously published works showing that basic metal oxides, including CaO, could act as promoters of this reaction [62]. Interestingly, these ketone compounds could also be considered valuable components of biofuels since they are quite stable during handling and storage. We would like to highlight the results found with

the Ca-based-1 catalyst in terms of aromatic content, as it was the only catalyst that led to a higher aromatic content than the non-catalytic co-pyrolysis run. For this catalyst, the aromatisation of olefins and hydrodeoxygenation of phenols may play a key role in the production of aromatics, particularly due to the intensification of H_2 production and the promotion of dehydration and cracking reactions in this catalyst. Given that the total basicity of the Ca-based-1 catalyst determined by the CO_2-TPD data was significantly lower than that determined for the other Ca-based catalysts, and the fact that this catalyst showed a pure CaO crystalline phase with marginal amount of impurities, it could be assumed that these properties of these catalysts could be key parameters facilitating the prevalence of aromatisation and hydrodeoxygenation routes over de-acidification and deoxygenation of the organic fraction through both ketonisation and esterification reactions. Accordingly, the higher content in ketones and esters obtained for the remaining Ca-based catalysts confirmed these assumptions. The main compounds identified after the catalytic process are shown in the supplementary data (Table S7).

At this point, it should be mentioned that although no regeneration cycles were performed in this study, a moderate deactivation of the catalyst by partial carbonation was expected according to previous tests at the pilot scale considering this type of catalysts [14]. This fact would make necessary the incorporation of a purge and input of fresh catalyst in order to maintain bio-oil quality. Fortunately, this purge would only slightly decrease the energy integration of the process, and the economic impact would also be moderate since this is inexpensive and widely available solid.

2.6. Char Characterisation

The solid fraction was also characterised in order to evaluate its potential as a solid fuel. Char produced by GS pyrolysis has a lower heating value (LHV) of 26.9 MJ/kg, whereas the char produced by WT pyrolysis showed an LHV of 30.9 MJ/kg. These values could be expected owing to the high carbon content in WT char fraction, and they were also in line with previous results [30]. At this point, it should be pointed out that the LHVs of the co-pyrolysis and catalytic co-pyrolysis chars were those theoretically expected, approximately 28 MJ/kg. These results confirmed the high potential of this product to be used for further energy purposes and to be used to support the heat requirements of the integrated process. Moreover, and in line with previous results in the fixed-bed reactor, a remarkable decrease in the sulphur content (0.5 wt%) was also achieved for all catalysts in comparison with the theoretically expected value (2.0 wt%). This could be expected since CaO is considered an ideal active solid for H_2S adsorption, forming CaS, and H_2O as products [63]. Thus, char desulphuration enhanced by the addition of Ca-based catalysts was also confirmed at this scale, as previously observed in the fixed bed reactor [30].

3. Materials and Methods

3.1. Biomass, Waste Tyres, and Catalysts

In this study, the biomass used was GSs (Vitis vinifera), obtained as a waste product of the wine industry in the north-east of Spain. The fresh biomass was dried to guarantee moisture levels below 2 wt% before being used directly. The WTs were received in the granulated form with particle sizes between 2 and 4 mm. WTs were supplied without the steel thread and textile netting. Table 7 summarises the main properties (proximate and ultimate analysis and heating value) of both feedstocks. The determination of these properties was carried out in accordance with standard methods [30]. As can be seen in Table 7, significant differences were apparent between the two raw materials. The high oxygen content (33.7 wt%) of GSs should be pointed out, which implies a low LHV (22.2 MJ/Kg), whereas WTs are characterised by high carbon content and low oxygen composition. It is worthy of mention that the heating values attributed to WTs are comparable to or even higher than the heating values characteristic of fossil fuels (% C: 87.9 wt%, % H: 3.3 wt%, LHV: 37 MJ/kg).

Table 7. Main properties of grape seeds and waste tyres.

	GSs [1]	WTs [2]
Ash (wt%)	4.3	3.8
Volatile matter (wt%)	65.1	63.6
Fixed Carbon (wt%)	24.3	31.8
Ultimate analysis (wt%)		
C	53.9	87.9
H	6.6	7.4
N	2.2	0.3
S	0.1	1.1
O	37.2	3.3
LHV (MJ/Kg)	20.5	37.0

[1]: Stabilised for 48 h at room temperature; [2]: As received.

In this study, four different Ca-based catalysts obtained from the calcination of low-cost limestone (Ca-based-1, Ca-based-2, Ca-based-3) and dolomite (Ca-based-4) were selected. Private companies situated in different regions of Europe supplied these solids. The Ca-based-1 catalyst was extracted from a German mine; the Ca-based-2 catalyst was excavated in the north of Spain; and, finally, the Ca-based-3 and Ca-based-4 catalyst samples were mined in the north-east of Spain. All solids were obtained after calcination at 900 °C. Particle size distribution for all solids was in the range of 300–600 μm.

X-ray diffraction (XRD), N_2-physisorption, mercury porosimetry, temperature-programmed desorption of ammonia (NH_3-TPD), temperature-programmed desorption of carbon dioxide (CO_2-TPD), and inductively coupled plasma-optical emission spectroscopy (ICP-OES) were also carried out to complete the characterisation of the catalysts. Experimental details related to XRD N_2-physisorption and mercury porosimetry techniques can be found elsewhere [64,65], and NH_3-TPD and CO_2-TPD determination have also been described by other authors [13].

3.2. Pilot Plant

Experiments were conducted in a pilot plant equipped with an auger reactor operating at atmospheric pressure. N_2 was used as the inert carrier gas. A detailed description of the pilot plant operation can be found in the supplementary information. The process flow diagram of this pilot plant is shown in Figure 4. This Auger reactor is able to process up to approximately 20 kg/h of GSs or WTs. The feeding system comprises two independent stirred hoppers to prevent the formation of voids, which can each be filled with approximately 25 kg of GSs or WTs. One hopper is used to feed the GS and WT mixture, and the other is used to feed the catalysts. Additionally, it should also be pointed out that catalysts were always diluted with an inert (sand), maintaining a (sand + catalyst) to feedstock ratio of 3:1. This stock of solids would be the minimum amount of heat carrier required for a self-sustainable process from an energy perspective [15]. In an integrated process, char combustion would be performed in a secondary reactor, providing the energy for the next pyrolysis step through the cycling of the heat carrier (sand + catalyst).

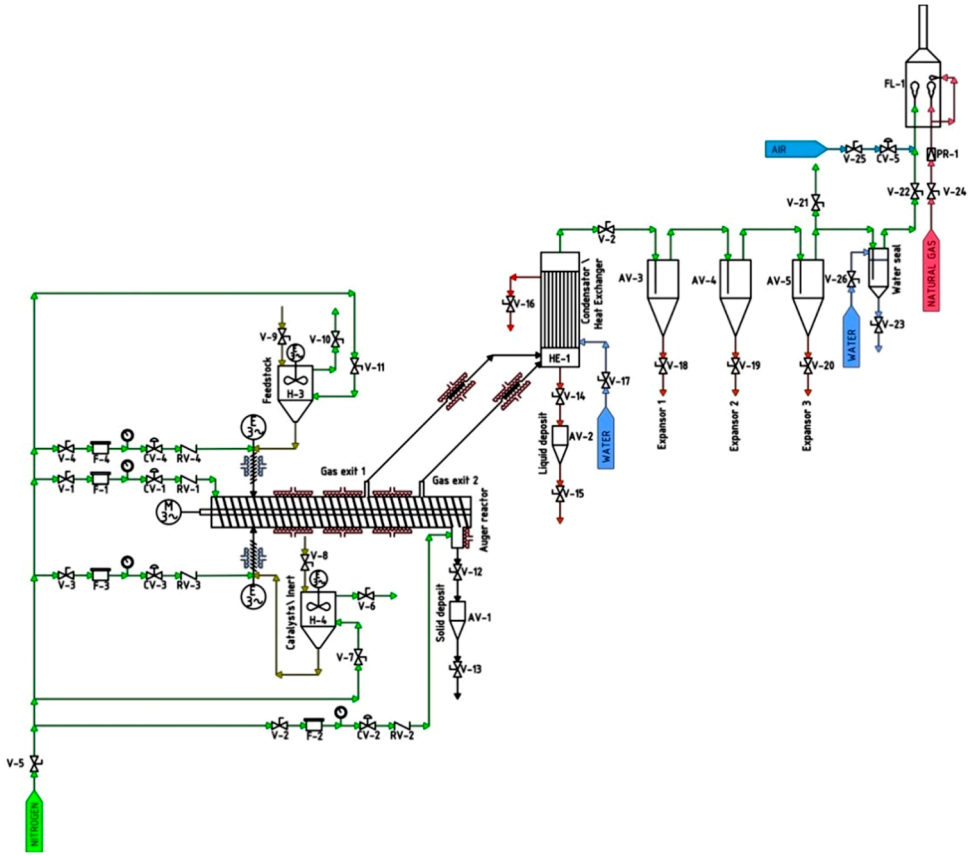

Figure 4. Process flow diagram of the pilot plant used for the catalytic co-pyrolysis experiments.

The reactor is surrounded by three independent electrical heating elements that provide the energy required to carry out the pyrolysis process. The converted product continuously leaves the reactor by gravity at the end of the reactor. The pyrolytic gas produced in the reactor is cooled in a shell and tubes condenser. Before flaring the gas, several samples were analysed by gas chromatography. The pilot plant is also provided with a control and acquisition system to monitor pressure by four pressure transducers and temperature by 10 thermocouples in different locations.

3.3. Catalysts Characterisation

A complete characterisation of the catalysts was carried out by means of XRD, ICP-OES, N_2 adsorption, and Hg porosimetry. The acidic characteristics of the Ca-based catalysts were studied by NH_3-TPD, and the basic characteristics of the catalysts were studied with TPD-CO_2. XRD patterns were measured with a Bruker D8 Advance series II diffractometer (Bruker, Delft, The Netherlands) using monochromatic Cu–Ka radiation (k = 0.1541 nm). Data were collected in the 2 h range from 5° to 80° using a scanning rate of 1°/min. The elemental composition of the different Ca-based catalysts (Al, Ca, Fe, Mg, K, Na, Si, Ti, P, Mn, and S) was determined by ICP-OES in a Perkin Elmer Optima 4300 system (Waltham, MA, Estados Unidos). N_2 physisorption was performed by a Quantachrome Autosorb 1 gas adsorption analyser (Graz, Austria). Prior to the adsorption measurements, the samples were outgassed in situ under a vacuum (4 mbar) at 250 °C for 4 h. The pore structure of the samples was determined by Hg porosimetry in a Micromeritics AutoPore V instrument (Norcross, GA, USA), according to the ISO 15901 standard. TPD techniques were measured by a Micromeritics Pulse Chemisorb 2700 instrument (Norcross, GA, USA) equipped with a thermal conductivity detector (TCD). Detailed information on the process conditions can be found in other research work [13].

3.4. Product Characterisation

The different products obtained after the process (liquid, solid, and gas) were characterised. Liquid and char yields were calculated by weight, and gas yield was calculated by balance. A heterogeneous liquid fraction was obtained, composed of two totally differentiable phases. The samples were centrifuged at 2000 rpm for 10 m, and the two liquid layers (organic/top and aqueous/bottom) were subsequently collected by a decantation process. The organic phase was then analysed in triplicate to determine different physicochemical properties, in accordance with standard methods. For the physical-chemical characterisation of the organic fraction, final composition, calorific value, water content, and pH were determined according to standard procedures [30], and density was determined by gravimetry. The GC-MS technique was also performed to analyse the chemical composition of the organic phase. Experimental details can be found in previous works [30]. The solid fraction was divided into char, CO_2, and coke yields for catalytic experiments. Yields of CO_2, and coke were directly calculated by the % of mass loss calculated from TGA experiments on each catalyst. The solid product (char) was also characterised by determining its calorific value and elemental analysis [30]. The non-condensable gas fraction was determined by GC using a TCD detector coupled to the Hewlett Packard II series [30,66]. Several thermogravimetric analyses were also performed in order to analyse catalyst carbonation.

4. Conclusions

The catalytic co-pyrolysis of both grape seeds and waste tyres using Ca-based catalysts was successfully performed in an Auger reactor at the pilot scale. The results demonstrated the great potential of this process for the production of an improved bio-oil. In general, a deoxygenated bio-oil with improved physical properties, such as viscosity and density, can be obtained using any low-cost Ca-based catalysts. More particularly, upgraded bio-oils can be practically dehydrated (H_2O content = 0.62 wt%) and fully deoxygenated (deoxygenation rate of ~95%), reaching heating values higher than 40 MJ/kg using a Ca-based catalyst with poor total basicity and a pure CaO crystalline phase without impurities. These properties seem to be key parameters that facilitate the prevalence of aromatisation and hydrodeoxygenation routes over the de-acidification and deoxygenation of the organic fraction through both ketonisation and esterification reactions, leading to a highly aromatic bio-oil. Moreover, due to the CO_2-capture and desulphuration effects inherent to these catalysts, a more environmentally friendly gas product was produced, generating H_2 and CH_4 as main components and, thus, increasing the range of potential applications for this fraction. Finally, the solid fraction was also shown to be a clean solid fuel to supply the energy for the proposed catalytic co-pyrolysis process.

Supplementary Materials: The following are available online at http://www.mdpi.com/2073-4344/9/12/992/s1, S.1 Pilot plant operation, Table S1: Yields after Catalytic experiments of GS and WT using Ca-based-1 catalyst, Table S2: Liquid properties after the catalytic experiments of GS and WT using Ca-based-1 catalyst, Table S3: Ultimate composition of the aqueous fraction after catalytic co-pyrolysis experiments, Table S4: Identified compounds (sorted by increasing retention time) in the liquid by GC/MS obtained after grape seeds pyrolysis, Table S5: Identified compounds (sorted by increasing retention time) in the liquid by GC/MS obtained after PS pyrolysis, Table S6: Identified compounds (sorted by increasing retention time) in the liquid by GC/MS obtained after co-pyrolysis of GS and WT experiments, Table S7: Identified compounds (sorted by increasing retention time) in the liquid by GC/MS obtained after Catalytic co-pyrolysis of GS and WT experiments, Table S8: Families and compounds identified after GC/MS.

Author Contributions: Conceptualization, T.G. and R.M.; methodology, O.S.-P., A.V. and J.M.L.; validation, O.S.-P. and A.V.; formal analysis O.S.-P. and A.V.; investigation, A.V., T.G. and R.M.; resources, T.G. and R.M.; data curation, O.S.-P. and A.V.; writing—original draft preparation, O.S.-P. and A.V.; writing—review and editing, T.G. and M.S.C.; supervision, T.G. and R.M.; project administration, T.G. and M.S.C.; funding acquisition, T.G. and R.M.

Funding: This research was funded by MINECO and FEDER for their financial support (Project ENE2015-68320-R) and the Regional Government of Aragon (DGA) under the research groups call.

Conflicts of Interest: The authors declare no conflict of interest.

References

1. Zheng, Y.; Tao, L.; Huang, Y.; Liu, C.; Wang, Z.; Zheng, Z. Improving aromatic hydrocarbon content from catalytic pyrolysis upgrading of biomass on a CaO/HZSM-5 dual-catalyst. *J. Anal. Appl. Pyrolysis* **2019**, *140*, 355–366. [CrossRef]
2. Imran, A.; Bramer, E.A.; Seshan, K.; Brem, G. An overview of catalysts in biomass pyrolysis for production of biofuels. *Biofuel Res. J.* **2018**, *5*, 872–885. [CrossRef]
3. Pires, A.P.P.; Arauzo, J.; Fonts, I.; Domine, M.E.; Arroyo, A.F.; Garcia-Perez, M.E.; Montoya, J.; Chejne, F.; Pfromm, P.; Garcia-Perez, M. Challenges and Opportunities for Bio-oil Refining: A Review. *Energy Fuels* **2019**. [CrossRef]
4. Oasmaa, A.; Van De Beld, B.; Saari, P.; Elliott, D.C.; Solantausta, Y. Norms, standards, and legislation for fast pyrolysis bio-oils from lignocellulosic biomass. *Energy Fuels* **2015**, *29*, 2471–2484. [CrossRef]
5. Stefanidis, S.D.; Kalogiannis, K.G.; Lappas, A.A. Co-processing bio-oil in the refinery for drop-in biofuels via fluid catalytic cracking. *Wiley Interdiscip. Rev.* **2018**, *7*. [CrossRef]
6. Thegarid, N.; Fogassy, G.; Schuurman, Y.; Mirodatos, C.; Stefanidis, S.; Iliopoulou, E.F.; Kalogiannis, K.; Lappas, A.A. Second-generation biofuels by co-processing catalytic pyrolysis oil in FCC units. *Appl. Catal. B Environ.* **2014**, *145*, 161–166. [CrossRef]
7. Baloch, H.A.; Nizamuddin, S.; Siddiqui, M.T.H.; Riaz, S.; Jatoi, A.S.; Dumbre, D.K.; Mubarak, N.M.; Srinivasan, M.P.; Griffin, G.J. Recent advances in production and upgrading of bio-oil from biomass: A critical overview. *J. Environ. Chem. Eng.* **2018**, *6*, 5101–5118. [CrossRef]
8. Yildiz, G.; Ronsse, F.; Duren, R.V.; Prins, W. Challenges in the design and operation of processes for catalytic fast pyrolysis of woody biomass. *Renew. Sustain. Energy Rev.* **2016**, *57*, 1596–1610. [CrossRef]
9. Dickerson, T.; Soria, J. Catalytic Fast Pyrolysis: A Review. *Energies* **2013**, *6*, 514–538. [CrossRef]
10. Rahman, M.M.; Liu, R.; Cai, J. Catalytic fast pyrolysis of biomass over zeolites for high quality bio-oil—A review. *Fuel Process. Technol.* **2018**, *180*, 32–46. [CrossRef]
11. Paasikallio, V.; Lindfors, C.; Kuoppala, E.; Solantausta, Y.; Oasmaa, A.; Lehto, J.; Lehtonen, J. Product quality and catalyst deactivation in a four day catalytic fast pyrolysis production run. *Green Chem.* **2014**, *16*, 3549–3559. [CrossRef]
12. Paasikallio, V.; Lindfors, C.; Lehto, J.; Oasmaa, A.; Reinikainen, M. Short vapour residence time catalytic pyrolysis of spruce sawdust in a bubbling fluidized-bed reactor with HZSM-5 catalysts. *Top. Catal.* **2013**, *56*, 800–812. [CrossRef]
13. Stefanidis, S.D.; Karakoulia, S.A.; Kalogiannis, K.G.; Iliopoulou, E.F.; Delimitis, A.; Yiannoulakis, H.; Zampetakis, T.; Lappas, A.A.; Triantafyllidis, K.S. Natural magnesium oxide (MgO) catalysts: A cost-effective sustainable alternative to acid zeolites for the in situ upgrading of biomass fast pyrolysis oil. *Appl. Catal. B Environ.* **2016**, *196*, 155–173. [CrossRef]
14. Veses, A.; Aznar, M.; Callén, M.S.; Murillo, R.; García, T. An integrated process for the production of lignocellulosic biomass pyrolysis oils using calcined limestone as a heat carrier with catalytic properties. *Fuel* **2016**, *181*, 430–437. [CrossRef]
15. Veses, A.; Aznar, M.; Martínez, I.; Martínez, J.D.; López, J.M.; Navarro, M.V.; Callén, M.S.; Murillo, R.; García, T. Catalytic pyrolysis of wood biomass in an auger reactor using calcium-based catalysts. *Bioresour. Technol.* **2014**, *162*, 250–258. [CrossRef] [PubMed]
16. Kalogiannis, K.G.; Stefanidis, S.D.; Karakoulia, S.A.; Triantafyllidis, K.S.; Yiannoulakis, H.; Michailof, C.; Lappas, A.A. First pilot scale study of basic vs. acidic catalysts in biomass pyrolysis: Deoxygenation mechanisms and catalyst deactivation. *Appl. Catal. B Environ.* **2018**, *238*, 346–357. [CrossRef]
17. Wong, S.L.; Ngadi, N.; Abdullah, T.A.T.; Inuwa, I.M. Current state and future prospects of plastic waste as source of fuel: A review. *Renew. Sustain. Energy Rev.* **2015**, *50*, 1167–1180. [CrossRef]
18. Abnisa, F.; Daud, W.M.A.W. A review on co-pyrolysis of biomass: An optional technique to obtain a high-grade pyrolysis oil. *Energy Convers. Manag.* **2014**, *87*, 71–85. [CrossRef]
19. Uzoejinwa, B.B.; He, X.; Wang, S.; El-Fatah Abomohra, A.; Hu, Y.; Wang, Q. Co-pyrolysis of biomass and waste plastics as a thermochemical conversion technology for high-grade biofuel production: Recent progress and future directions elsewhere worldwide. *Energy Convers. Manag.* **2018**, *163*, 468–492. [CrossRef]
20. Alvarez, J.; Amutio, M.; Lopez, G.; Santamaria, L.; Bilbao, J.; Olazar, M. Improving bio-oil properties through the fast co-pyrolysis of lignocellulosic biomass and waste tyres. *Waste Manag.* **2019**, *85*, 385–395. [CrossRef]

21. Wang, J.; Zhong, Z.; Ding, K.; Li, M.; Hao, N.; Meng, X.; Ruan, R.; Ragauskas, A.J. Catalytic fast co-pyrolysis of bamboo sawdust and waste tire using a tandem reactor with cascade bubbling fluidized bed and fixed bed system. *Energy Convers. Manag.* **2019**, *180*, 60–71. [CrossRef]
22. Shah, S.A.Y.; Zeeshan, M.; Farooq, M.Z.; Ahmed, N.; Iqbal, N. Co-pyrolysis of cotton stalk and waste tire with a focus on liquid yield quantity and quality. *Renew. Energy* **2019**, *130*, 238–244. [CrossRef]
23. Van Nguyen, Q.; Choi, Y.S.; Choi, S.K.; Jeong, Y.W.; Kwon, Y.S. Improvement of bio-crude oil properties via co-pyrolysis of pine sawdust and waste polystyrene foam. *J. Environ. Manag.* **2019**, *237*, 24–29. [CrossRef] [PubMed]
24. Brebu, M.; Yanik, J.; Uysal, T.; Vasile, C. Thermal and catalytic degradation of grape seeds/polyethylene waste mixture. *Cellul. Chem. Technol.* **2014**, *48*, 665–674.
25. Izzatie, N.I.; Basha, M.H.; Uemura, Y.; Hashim, M.S.M.; Afendi, M.; Mazlan, M.A.F. Co-pyrolysis of rubberwood sawdust (RWS) and polypropylene (PP) in a fixed bed pyrolyzer. *J. Mech. Eng. Sci.* **2019**, *13*, 4636–4647. [CrossRef]
26. Martínez, J.D.; Veses, A.; Mastral, A.M.; Murillo, R.; Navarro, M.V.; Puy, N.; Artigues, A.; Bartrolí, J.; García, T. Co-pyrolysis of biomass with waste tyres: Upgrading of liquid bio-fuel. *Fuel Process. Technol.* **2014**, *119*, 263–271. [CrossRef]
27. Hassan, H.; Lim, J.K.; Hameed, B.H. Recent progress on biomass co-pyrolysis conversion into high-quality bio-oil. *Bioresour. Technol.* **2016**, *221*, 645–655. [CrossRef]
28. Zhang, X.; Lei, H.; Chen, S.; Wu, J. Catalytic co-pyrolysis of lignocellulosic biomass with polymers: A critical review. *Green Chem.* **2016**, *18*, 4145–4169. [CrossRef]
29. Zhang, L.; Bao, Z.; Xia, S.; Lu, Q.; Walters, K.B. Catalytic pyrolysis of biomass and polymer wastes. *Catalysts* **2018**, *8*, 659. [CrossRef]
30. Sanahuja-Parejo, O.; Veses, A.; Navarro, M.V.; López, J.M.; Murillo, R.; Callén, M.S.; García, T. Catalytic co-pyrolysis of grape seeds and waste tyres for the production of drop-in biofuels. *Energy Convers. Manag.* **2018**, *171*, 1202–1212. [CrossRef]
31. Iftikhar, H.; Zeeshan, M.; Iqbal, S.; Muneer, B.; Razzaq, M. Co-pyrolysis of sugarcane bagasse and polystyrene with ex-situ catalytic bed of metal oxides/HZSM-5 with focus on liquid yield. *Bioresour. Technol.* **2019**, *289*, 121647. [CrossRef] [PubMed]
32. Wang, J.; Jiang, J.; Zhong, Z.; Wang, K.; Wang, X.; Zhang, B.; Ruan, R.; Li, M.; Ragauskas, A.J. Catalytic fast co-pyrolysis of bamboo sawdust and waste plastics for enhanced aromatic hydrocarbons production using synthesized CeO2/γ-Al2O3 and HZSM-5. *Energy Convers. Manag.* **2019**, *196*, 759–767. [CrossRef]
33. Mishra, R.K.; Iyer, J.S.; Mohanty, K. Conversion of waste biomass and waste nitrile gloves into renewable fuel. *Waste Manag.* **2019**, *89*, 397–407. [CrossRef] [PubMed]
34. Ding, K.; Zhong, Z.; Wang, J.; Zhang, B.; Fan, L.; Liu, S.; Wang, Y.; Liu, Y.; Zhong, D.; Chen, P.; et al. Improving hydrocarbon yield from catalytic fast co-pyrolysis of hemicellulose and plastic in the dual-catalyst bed of CaO and HZSM-5. *Bioresour. Technol.* **2018**, *261*, 86–92. [CrossRef]
35. Zhang, B.; Zhong, Z.; Chen, P.; Ruan, R. Microwave-assisted catalytic fast co-pyrolysis of Ageratina adenophora and kerogen with CaO and ZSM-5. *J. Anal. Appl. Pyrolysis* **2017**, *127*, 246–257. [CrossRef]
36. Gulab, H.; Hussain, K.; Malik, S.; Hussain, Z.; Shah, Z. Catalytic co-pyrolysis of Eichhornia Crassipes biomass and polyethylene using waste Fe and $CaCO_3$ catalysts. *Int. J. Energy Res.* **2016**, *40*, 940–951. [CrossRef]
37. Liu, S.; Xie, Q.; Zhang, B.; Cheng, Y.; Liu, Y.; Chen, P.; Ruan, R. Fast microwave-assisted catalytic co-pyrolysis of corn stover and scum for bio-oil production with CaO and HZSM-5 as the catalyst. *Bioresour. Technol.* **2016**, *204*, 164–170. [CrossRef]
38. Treedet, W.; Suntivarakorn, R. Design and operation of a low cost bio-oil fast pyrolysis from sugarcane bagasse on circulating fluidized bed reactor in a pilot plant. *Fuel Process. Technol.* **2018**, *179*, 17–31. [CrossRef]
39. Campuzano, F.; Brown, R.C.; Martínez, J.D. Auger reactors for pyrolysis of biomass and wastes. *Renew. Sustain. Energy Rev.* **2019**, *102*, 372–409. [CrossRef]
40. Martínez, J.D.; Murillo, R.; García, T.; Veses, A. Demonstration of the waste tire pyrolysis process on pilot scale in a continuous auger reactor. *J. Hazard. Mater.* **2013**, *261*, 637–645. [CrossRef]
41. Veses, A.; Aznar, M.; López, J.M.; Callén, M.S.; Murillo, R.; García, T. Production of upgraded bio-oils by biomass catalytic pyrolysis in an auger reactor using low cost materials. *Fuel* **2015**, *141*, 17–22. [CrossRef]
42. Brassard, P.; Godbout, S.; Raghavan, V. Pyrolysis in auger reactors for biochar and bio-oil production: A review. *Biosyst. Eng.* **2017**, *161*, 80–92. [CrossRef]

43. Lan, Y.; Niu, D.; Liu, Q.; Yang, J.; Yang, Q.; Xu, J. Briquetting burnt dolomite powder for recycling in steel plants. *Nat. Environ. Pollut. Technol.* **2014**, *13*, 649–652.
44. Chinthakuntla, D.; Kumar, M.K.; Chakra, C.S.; Rao, K.; Dayakar, T. Calcium Oxide Nano Particles Synthesized From Chicken Egg Shells by Physical Method. In Proceedings of the International Conference on Emerging Technologies in Mechanical Sciences, Hyderabad, India, 26–27 December 2014.
45. Linggawati, A. Preparation and Characterization of Calcium Oxide Heterogeneous Catalyst Derived from Anadara Granosa Shell for Biodiesel Synthesis. *KnE Eng.* **2016**, *1*. [CrossRef]
46. Lee, S.L.; Wong, Y.C.; Tan, Y.P.; Yew, S.Y. Transesterification of palm oil to biodiesel by using waste obtuse horn shell-derived CaO catalyst. *Energy Convers. Manag.* **2015**, *93*, 282–288. [CrossRef]
47. Correia, L.M.; de Sousa Campelo, N.; Novaes, D.S.; Cavalcante, C.L.; Cecilia, J.A.; Rodríguez-Castellón, E.; Vieira, R.S. Characterization and application of dolomite as catalytic precursor for canola and sunflower oils for biodiesel production. *Chem. Eng. J.* **2015**, *269*, 35–43. [CrossRef]
48. Dabros, T.M.H.; Stummann, M.Z.; Høj, M.; Jensen, P.A.; Grunwaldt, J.D.; Gabrielsen, J.; Mortensen, P.M.; Jensen, A.D. Transportation fuels from biomass fast pyrolysis, catalytic hydrodeoxygenation, and catalytic fast hydropyrolysis. *Prog. Energy Combust. Sci.* **2018**, *68*, 268–309. [CrossRef]
49. Rahman, M.; Chai, M.; Sarker, M.; Nishu; Liu, R. Catalytic pyrolysis of pinewood over ZSM-5 and CaO for aromatic hydrocarbon: Analytical Py-GC/MS study. *J. Energy Inst.* **2019**. [CrossRef]
50. Chen, X.; Li, S.; Liu, Z.; Chen, Y.; Yang, H.; Wang, X.; Che, Q.; Chen, W.; Chen, H. Pyrolysis characteristics of lignocellulosic biomass components in the presence of CaO. *Bioresour. Technol.* **2019**, *287*. [CrossRef]
51. Chen, X.; Chen, Y.; Yang, H.; Wang, X.; Che, Q.; Chen, W.; Chen, H. Catalytic fast pyrolysis of biomass: Selective deoxygenation to balance the quality and yield of bio-oil. *Bioresour. Technol.* **2019**. [CrossRef]
52. Hossain, A.K.; Davies, P.A. Pyrolysis liquids and gases as alternative fuels in internal combustion engines—A review. *Renew. Sustain. Energy Rev.* **2013**, *21*, 165–189. [CrossRef]
53. Biradar, C.H.; Subramanian, K.A.; Dastidar, M.G. Production and fuel quality upgradation of pyrolytic bio-oil from Jatropha Curcas de-oiled seed cake. *Fuel* **2014**, *119*, 81–89. [CrossRef]
54. de Luna, M.D.G.; Cruz, L.A.D.; Chen, W.H.; Lin, B.J.; Hsieh, T.H. Improving the stability of diesel emulsions with high pyrolysis bio-oil content by alcohol co-surfactants and high shear mixing strategies. *Energy* **2017**, *141*, 1416–1428. [CrossRef]
55. Cao, Q.; Jin, L.; Bao, W.; Lv, Y. Investigations into the characteristics of oils produced from co-pyrolysis of biomass and tire. *Fuel Process. Technol.* **2009**, *90*, 337–342. [CrossRef]
56. Li, J.J.; Zhou, T.D.; Tang, X.D.; Chen, X.D.; Zhang, M.; Zheng, X.P.; Wang, C.S.; Deng, C.L. Viscosity reduction process of heavy oil by catalytic co-pyrolysis with sawdust. *J. Anal. Appl. Pyrolysis* **2019**, *140*, 444–451. [CrossRef]
57. Persson, H.; Yang, W. Catalytic pyrolysis of demineralized lignocellulosic biomass. *Fuel* **2019**, *252*, 200–209. [CrossRef]
58. Thoharudin, T.; Nadjib, M.; Santosa, T.H.A.; Juliansyah; Zuniardi, A.; Shihabudin, R. Properties of co-pyrolysed palm kernel shell and plastic grocery bag with CaO as catalyst. In Proceedings of the 3rd International Conference on Biomass: Accelerating the Technical Development and Commercialization for Sustainable Bio-based Products and Energy, Bogor, Indonesia, 1–2 August 2018.
59. Sukumar, V.; Manieniyan, V.; Senthilkumar, R.; Sivaprakasam, S. Production of bio oil from sweet lime empty fruit bunch by pyrolysis. *Renew. Energy* **2020**, *146*, 309–315. [CrossRef]
60. Ghorbannezhad, P.; Kool, F.; Rudi, H.; Ceylan, S. Sustainable production of value-added products from fast pyrolysis of palm shell residue in tandem micro-reactor and pilot plant. *Renew. Energy* **2020**, *145*, 663–670. [CrossRef]
61. Vichaphund, S.; Wimuktiwan, P.; Sricharoenchaikul, V.; Atong, D. In situ catalytic pyrolysis of Jatropha wastes using ZSM-5 from hydrothermal alkaline fusion of fly ash. *J. Anal. Appl. Pyrolysis* **2019**, *139*, 156–166. [CrossRef]
62. Hussmann, G.P.; AMOCO Corporation. Preparation of dialkyl ketones from aliphatic carboxylic acids. U.S. Patent 4754074A, 28 June 1988.
63. Choi, G.-G.; Oh, S.-J.; Kim, J.-S. Scrap tire pyrolysis using a new type two-stage pyrolyzer: Effects of dolomite and olivine on producing a low-sulfur pyrolysis oil. *Energy* **2016**, *114*, 457–464. [CrossRef]

64. Veses, A.; Puértolas, B.; Callén, M.S.; García, T. Catalytic upgrading of biomass derived pyrolysis vapors over metal-loaded ZSM-5 zeolites: Effect of different metal cations on the bio-oil final properties. *Microporous Mesoporous Mater.* **2015**, *209*, 189–196. [CrossRef]
65. Puértolas, B.; Veses, A.; Callén, M.S.; Mitchell, S.; García, T.; Pérez-Ramírez, J. Porosity-Acidity Interplay in Hierarchical ZSM-5 Zeolites for Pyrolysis Oil Valorization to Aromatics. *ChemSusChem* **2015**, *8*, 3283–3293. [CrossRef] [PubMed]
66. Sanahuja-Parejo, O.; Veses, A.; Navarro, M.V.; López, J.M.; Murillo, R.; Callén, M.S.; García, T. Drop-in biofuels from the co-pyrolysis of grape seeds and polystyrene. *Chem. Eng. J.* **2018**. [CrossRef]